Journal of Molecular Catalysis A: Chemical 349 (2011) 55–62

Contents lists available at SciVerse ScienceDirect

Journal of Molecular Catalysis A: Chemical

journal homepage: www.elsevier.com/locate/molcata

Sun light assisted photocatalytic decontamination of sulfur mustard using ZnO nanoparticles

G.K. Prasad*, P.V.R.K. Ramacharyulu, Beer Singh, K. Batra, Anchal R. Srivastava, K. Ganesan, R. Vijayaraghavan

Defence Research and Development Establishment, Jhansi Road, Gwalior, India

ARTICLE INFO

Article history:
Received 16 June 2011
Received in revised form 4 August 2011
Accepted 19 August 2011
Available online 27 August 2011

Keywords:
Sun light
Sulfur mustard
ZnO nanoparticles
Decontamination
Photocatalysis

ABSTRACT

Sun light assisted photocatalytic decontamination of sulfur mustard (HD) was studied by using ZnO nanoparticles and the data was compared with those carried out in the presence of UVA and visible light radiation. In the presence of Sun light, 100% of HD was decontaminated in 12 h. Whereas, in the presence of UVA light 90%, and in visible light 80% of HD was decontaminated in 12 h. GC–MS data indicated the formation of thiodiglycol, hemisulfur mustard, divinyl sulfide, 2-chloro ethyl vinyl sulfide, etc., on the surface of ZnO nanoparticles in the case of dark and visible light irradiation experiments. However, in Sun light and UVA light irradiation experiments, GC–MS data indicated the formation of HD sulfoxide, HD sulfone, 1,3-dithiane, 2-chloro ethanol, acetaldehyde, carbon dioxide, etc. along with hydrolysis and elimination products. Under the illumination of visible light and in dark hydrolysis, elimination and surface complexation reactions have contributed to decontamination of HD. Whereas, in the presence of Sun light and UVA light, photocatalytic reactions like C–S bond cleavage, oxidation of C, S atoms were observed to have contributed to decontamination of HD in addition to hydrolysis and elimination reactions.

1. Introduction

Decontamination of surface tainted with chemical warfare agents (CWA) is the prerequisite act we do to avoid health hazards. Sulfur mustard, a well known CWA, causes damage to skin, eyes and respiratory system. It alkylates purines in DNA, damages dermal–epidermal junction, causes swelling of space between dermis and basal cells due to fluid accumulation and lead to blistering. It was used for first time on 12th July, 1917 at city Ypers, France by German forces on British forces. Due to its effectiveness, persistency and stability, it has been termed as king of CWA. Undesirable health effects caused by sulfur mustard (HD) contact can be avoided by its decontamination [1].

Nanosized metal oxides such as Al_2O_3, MgO, CaO, ZnO, TiO_2, and mixed oxides of alumina [2–10], titania nanotubes [11], metal ion exchanged titania nanotubes [12], zinc oxide nanorods [13], manganese oxide nanostructures [14–16] have been tested recently as potential sorbent decontaminants against CWA. Due to high surface area, large numbers of reactive edges, corner defect sites, unusual lattice planes and high surface area-to-volume ratio, acid and base sites, surface hydroxyl groups, nanocrystalline metal oxides possess enhanced sorptive and reactive properties towards CWAs and these in turn help in decontamination.

On the other hand, heterogeneous photocatalysis is a gifted alternative approach for decontamination of CWA. Heterogeneous photocatalysis using nano-sized photocatalysts is more interesting due to their exceptional properties [17]. Because of high surface area-to-volume ratio, nano-photocatalysts facilitate adsorption of more amount of CWA molecules on their surface due to inherited large adsorption capacity, and assist in high photocatalytic conversion of CWA. When a semiconductor material is irradiated with radiation whose energy is greater than band gap, electron–hole pairs are generated. These e^-–h^+ pairs react with moisture and surrounding oxygen species to form hydroxyl radicals (•OH) and superoxide anion ($O_2^{-\bullet}$) radicals. Surface migrated electrons and holes, hydroxyl radicals, superoxide anion radicals react with adsorbed pollutant molecules like CWA and render them non-toxic [18–21]. Recent studies have focussed mainly on photocatalytic oxidation of CWA assisted by TiO_2 particles. Vorontsov and co workers have extensively studied photocatalytic decontamination of organophosphorous CWAs using TiO_2 particles both in liquid and

* Corresponding author. Tel.: +91 751 2390169; fax: +91 751 2233482.
E-mail addresses: gkprasad@lycos.com, gkprasad2001@yahoo.com (G.K. Prasad).

1381-1169/$ – see front matter © 2011 Elsevier B.V. All rights reserved.
doi:10.1016/j.molcata.2011.08.018

gas phases. They also have studied the photocatalytic decontamination of 2-chloro ethyl ethyl sulfide (CEES), a simulant of HD using titania materials of large particle size. As per his observations, CEES degraded to its oxidation products due to photocatalysis [22–26].

While most of the researchers concentrated on TiO_2 as photocatalyst plenitude of studies have also been focussed to explore potential of other metal oxides for the degradation of environmental pollutants [27,28]. Among others, zinc oxide appears as promising photocatalyst, and quantum efficiency of ZnO powder is significantly greater than that of TiO_2 powder and in some cases, ZnO has proven to be more effective than TiO_2 [29,30]. In addition to these, ZnO is available at low cost, which gives it an important advantage. ZnO mediated photocatalysis process under UV light radiation has been successfully used to degrade dye pollutants for the past few years [31]. However, solar UV light reaching surface of earth which is available to excite TiO_2 is relatively small (around 4%), and artificial UV-light sources are somewhat expensive. The biggest advantage of ZnO is that it absorbs over a larger fraction of solar spectrum than TiO_2 [32,33].

On the other hand, ZnO was found to be promising adsorbent for the degradation of environmental pollutants in the presence of light. It was used as a photocatalyst for degradation of terephthalic acid (TPA), a toxic contaminant in textile industry [34]. It was also used for degradation of salicylic acid, a water pollutant which arises from a number of sources including paper milling, cosmetic industries [35]. In addition to these, ZnO powders were also exploited for their photocatalytic activities in degradation of methyl orange dye [36]. Recently, Prasad et al. have studied and reported the detoxification reactions of HD on the surface of zinc oxide nanorods and explored role of hydrolysis and elimination reactions in its detoxification [37]. They have studied decontamination of sarin on ZnO nanoparticles [38]. However, no body have studied photoassisted decontamination of CWA like HD. Inspired by the above, we have synthesized the nanomaterials of ZnO by sol–gel method and attempted to study photocatalytic decontamination reactions of HD in the presence of Sun light and compared the data with that carried out in UVA and visible light radiations. Prior to the reaction studies, nanocrystalline materials were characterized by TEM, XRD, FT-IR, TGA, N_2 BET, etc.

2. Experimental

2.1. Materials

Zinc acetate dihydrate, oxalic acid dihydrate, dichloromethane, ethyl acetate, dimethyl sulfoxide, and methanol were obtained from M/s. S.D fine chemical India Ltd., and ethanol was purchased from E. Merck India Ltd. HD was synthesized in our laboratory and it is highly toxic and should be handled in a fume cupboard (with a proper scrubbing/filtration system) by trained persons with personal protective measures.

2.2. Synthesis of zinc oxide nanomaterials

Zinc oxide nanomaterials were synthesized by sol–gel method [39]. For this purpose, methanolic solution of oxalic acid was added to hot methanolic zinc acetate solution in a conventional reaction flask with a constant heating and stirring. The reaction temperature was maintained at 60 °C throughout addition of above reactants. Thereafter, obtained materials were filtered, dried at 80 °C and calcined at 500 °C. To obtain materials of other crystallite sizes, xero-gel was calcined at 900 °C, 1000 °C and 1100 °C temperatures respectively.

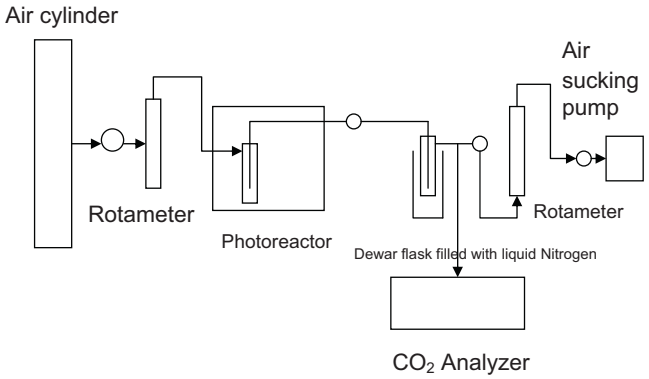

Fig. 1. Schematic diagram of the experimental set up.

2.3. Photocatalyitc degradation of HD

100 mg of ZnO was taken in a quartz tube and 100 μl of dichloromethane solution containing 2 μl of HD was spiked on it and dichloromethane was allowed to evaporate. Subsequently, quartz tube containing the nano photocatalyst was irradiated by UVA or visible light or Sun light in a photo reactor. M/s. Luzchem, Canada of LZC 4V model photo reactor was used for UVA light and visible light irradiation experiments. Intensity of light was measured by digital light meter (SLM 110 model) of A.W. Sperry Instruments, USA with help of adopters provided. Intensity of UVA light (~360 nm) was found to be 0.3 mW/cm^2 and intensity of visible light (> 450 nm) was found to be 18 mW/cm^2. A constant airflow @ 150 ml/min was passed into the photo reactor from air cylinder of high purity. Experimental setup designed for this analysis is shown in Fig. 1.

The gaseous products formed on surface of catalyst when irradiated with light were trapped by suction through liquid nitrogen trap @ 40 ml/min. The trapped solution was analyzed for CO_2 and CH_3CHO. CO_2 was analyzed by the equipment from Technovation India Ltd., India, and CH_3CHO was analyzed by NUCON GC fitted with FID detector by using OV-17 packed column of length 1 m in an isothermal mode as mentioned above. Remaining HD was extracted after periodic intervals of time using acetonitrile. The extracted samples were analyzed with GC affixed with FID detector for monitoring products as well as remaining HD. UVA lights, fluorescent tubes of Luzchem, Canada were used for this study. For Sun light irradiation studies, experiments were conducted by using test rig shown in Fig. 1. Samples were exposed to Sun light by keeping thin glass plate on the reactor. After keeping the samples inside, the reactor was closed as in Fig. 1.

2.4. Characterization

XRD patterns were obtained in an XPert Pro Diffractometer, Panalytical, Netherlands, using Cu Kα radiation. N_2 BET measurements were done on ASAP 2020 of Micromeritics, USA. Subsequently, thermograms were recorded on TGA-2950, TA instruments, USA. HP Agilent GC–MS system (5973 Inert) was used for the characterization of reaction products. Transmission electron microscopy measurements were done on Tecnai transmission electron microscope of FEI make. Samples were suspended in 30 ml acetone, and then suspension was sonicated for 30 min. After that, suspension was placed on carbon coated copper grids of 3 mm dia and dried at room temperature prior to the analysis.

Table 1
BET surface area and pore volume values of ZnO particles synthesized by calcination of xerogel at 500 °C, 900 °C, 1000 °C, and 1100 °C.

Calcination temperature of the xerogel (°C)	BET surface area (m^2/g)	Total pore volume (ml/g)
500	42.6	0.15
900	33.4	0.12
1000	18.1	0.04
1100	6.78	0.02

3. Results and discussion

Crystallite sizes of ZnO particles prepared by calcination of the xerogel at 500 °C, 900 °C, 1000 °C, and 1100 °C were determined by TEM. TEM image of ZnO particles obtained by calcination at 500 °C illustrated the crystallites with ~30 nm size (Fig. 2(a)). Whereas, image of ZnO particles obtained by calcination of the gel at 900 °C (Fig. 2(b)), 1000 °C (Fig. 2(c)) showed the crystallites with sizes at around 300–500 nm, ~1000 nm respectively. The crystallite size of the ZnO particles obtained by calcination at 1100 °C was found to be ~2000 nm. Morphology of the ZnO nanoparticles influences the chemical reactivity to a noticeable extent. TEM data also show the formation of ZnO particles of various sizes with spherical shape. It also shows the randomly oriented aggregates of spherical sized nanoparticles and these aggregates were found to be having sizes ranging from 30 nm to 2000 nm. Growth of the crystallite size with increased calcination temperature can be ascribed to sintering of particles at high temperatures. In addition to this, they were found to be self assembled in peculiar and random manner to form chain like aggregates with porous structure. Perhaps, the surface charges and structural similarity observed to have facilitated formation of these self assembled chain like nanostructures.

XRD data of the obtained materials, calcined at various temperatures such as 500 °C, 900 °C, 1000 °C, and 1100 °C depicted peaks at 2θ values 31.775°, 34.425°, 36.275° and 47.625°. These peaks can be attributed to the presence of (1 0 0), (0 0 2), (1 0 1) and (0 0 2) indices. This XRD pattern (Fig. 3) illustrates 2θ values and relative intensities of peaks that match with JCPDS data of zincite (see Fig. 3).

Surface area of adsorbent materials influences their chemical reactivity to a greater extent, as adsorption capacity directly depends on surface area values. For this purpose, obtained ZnO nanoparticles were subjected to N_2 BET analysis. The values of surface area and pore volume are incorporated in Table 1. As the crystallite size was reduced from 2000 nm to 30 nm, value of surface area was seemed to increase.

3.1. Photocatalyitc degradation of HD

Sunlight (250–800 nm) or UVA light (320–400 nm) or visible light (400–800 nm) when used alone demonstrated negligible decontamination efficiency towards HD as indicated by blank experiments conducted in absence of nano ZnO particles. This observation can be attributed to the fact that, photon energy of the above mentioned light radiations is not enough to excite HD molecule. In order to investigate the reactivity of nano ZnO particles in dark, experiments were carried out by using particles of 30 nm size. Apparently, they have decontaminated 57% of HD within 16 h. This reactive decontamination property of nano ZnO towards HD in the absence of light can be ascribed to available surface area on nanoparticles, surface hydroxyl groups, Lewis acid sites, moisture which was present over the surface of nanoparticles. In addition to these, with decrease in average crystallite size of ZnO nanoparticles decontamination efficiency was found to increase. When crystallite size was reduced from 2000 nm to 30 nm, the decontamination efficiency was found to increase from 8 to 57% within 16 h. The increased decontamination efficiency with decreased crystallite

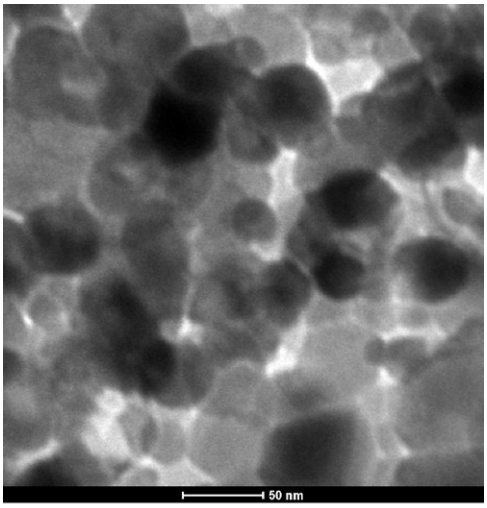

(a)

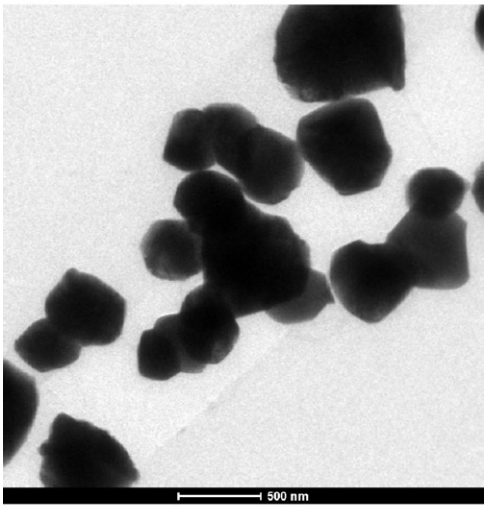

(b)

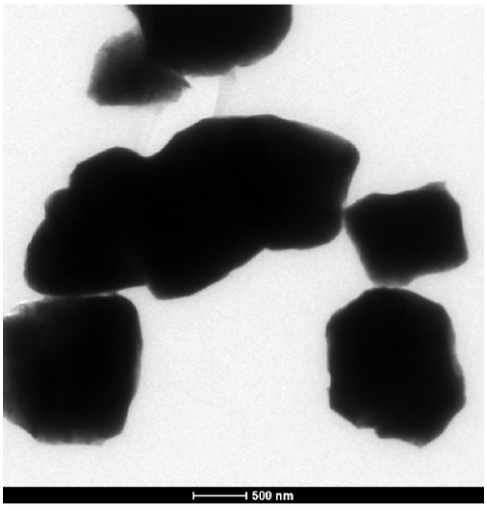

(c)

Fig. 2. TEM images of the ZnO particles calcined at 500 °C (a), 900 °C (b), and 1000 °C (c).

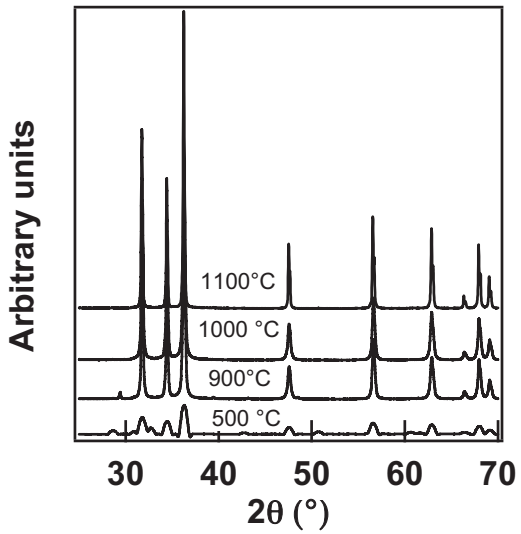

Fig. 3. XRD data of ZnO particles obtained by calcination at various temperatures.

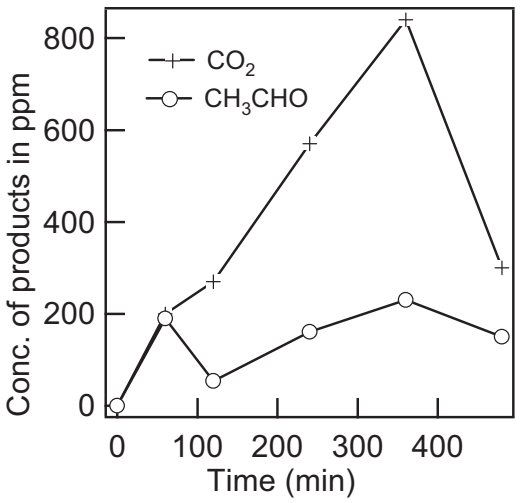

Fig. 4. Product concentration profile of HD decontaminated on nano ZnO irradiated with Sun light.

size can be credited to increased surface area-to-volume ratio, and increased number of reactive sites and surface hydroxyl groups.

GC–MS data of extracted samples indicated formation of thiodiglycol (*m*/*z* values 122, 104, 91, 61, 43) and hemisulfur mustard (*m*/*z* values 140, 141, 111, 109, 104, 73, 63, 45, 27, 29). These products attributed decontamination of HD through hydrolysis reactions. Besides these, certain elimination products of HD were also detected such as divinyl sulfide, vinyl chloro ethyl sulfide, and vinyl hydroxyl ethyl sulfide and showed the *m*/*z* values of 85, 71, 59 and 53; 122, 73, 60, 57 and 53; and 104, 73, 61 and 59, respectively.

It was observed that, reactions of HD with ZnO nanoparticles in the absence of light were found to be very slow, contributed only to hydrolysis, elimination and surface complexation reactions. The samples were found to contain 1–3% moisture content and presumably could have contributed to hydrolysis of HD. As the reactions were found to be slow, heterogeneous photocatalytic process assisted by ZnO nanoparticles was opted to facilitate faster decontamination of HD. Moreover, decontamination of HD facilitated by nano-ZnO and Sun light will be very interesting as nano ZnO can be sprayed on contaminated surfaces, and synchronized photocatalysis assisted by Sun light and nano ZnO can take care of contaminants, finally contaminated surfaces are rendered safe to operate.

In order to understand the reactivity of ZnO nanoparticles towards HD in the presence of Sun light, experiments were carried out using the particles with average crystallite size of 30 nm. 100% of HD was found to get decontaminated in 12 h indicating the photocatalytic decontamination of HD. Owing to increased adsorption capacity, more number of HD molecules were found to be adsorbed on surface of ZnO nanoparticles and reacted with electrons and holes that were generated on its surface upon illumination with Sun light. In addition to this, holes reacted with moisture to form hydroxyl radicals (•OH) and protons, while electrons reacted with oxygen to form superoxide anion ($O_2^{-\bullet}$) radicals. These $O_2^{-\bullet}$ and •OH are extremely unstable and have reacted with adsorbed HD molecules and decontaminated it to various reaction products. Collectively in the presence of Sun light, nano ZnO had caused decontamination of HD through hydrolysis, elimination as well as photocatalytic reactions.

Acetaldehyde and carbon dioxide were the gaseous products formed in large quantities as indicated by GC–MS data. The carbon dioxide concentration increased gradually with time and approached a value of 840 ppm in 6 h and started decreasing, and finally reached to 300 ppm in 8 h due to degradation of HD molecule (Fig. 4).

On the other hand, rate of CO_2 generation should be increased, however, because of the gradual increase in amount of acetaldehyde formed, which was further converted to acetic acid, and then to CO_2 and H_2O, significant quantity of CO_2 was not observed. Incomplete degradation of surface organic compounds could have also caused low CO_2 concentration. This observation can be attributed to oxidation of carbon atom of HD. The concentration of CH_3CHO had reached a maximum value of 220 ppm in 6 h and started decreasing, indicating the deactivation of catalyst and poisoning of surface, formation of HCl and H_2SO_4 on the surface. Less volatile products formed on the surface of nano ZnO were studied by extracting with dry acetonitrile, ethyl acetate and dichloromethane. The solution was analyzed by GC–MS after silylation. GC–MS depicted the formation of bis(2-chloroethyl) disulfide $(-SC_2H_4Cl)_2$. It seemed that, thiyl radicals $ClCH_2CH_2S^\bullet$ were formed due to photo reaction recombined giving the detected product bis(2-chloroethyl) disulfide $(-SC_2H_4Cl)_2$. In addition to these, some other dimerized products were also recorded by GC–MS (Table 2). This observation can be ascribed to cleavage of C–S bond due to photocatalysis.

Moreover, several other products were also detected by GC–MS and the data was similar to that observed in the case of photocatalytic decomposition of 2-chloro ethyl ethyl sulfide on TiO_2 [26]. Hemisulfur mustard and thiodiglycol were seemed to be formed due to hydrolysis of HD and were detected by GC–MS analysis of silylated extract of ethyl acetate from ZnO surface. In addition to these, 2,2-dichloro diethyl sulphoxide, 2,2-dichloro diethyl sulfone, 1,3-oxathiolane, etc., were also detected in acetonitrile extract. However, 2-chloro ethyl vinyl sulfide, vinyl chloride, acetic acid, 2-chloro ethanol, etc. were the minor products observed in ethyl acetate extract. Of all illumination experiments, Sun light assisted photocatalysis by ZnO has exhibited superior decontamination efficiency towards HD. Hence, we have studied effect of average crystallite size on photocatalytic decontamination efficiency. It was observed that, as crystallite size decreased from 2000 nm to 30 nm the decontamination efficiency increased from 84% to 95% in 8 h.

In addition to the above, data obtained for the experiments carried out in Sun light illumination was compared with that obtained for visible light as well as UVA light.

In the presence of visible light of 18 mW/cm^2 intensity, experiments were carried out using nano ZnO particles with average crystallite size of 30 nm. It was observed that, 93% of HD was

Table 2
List of products detected due to the photocatalytic decontamination of HD on nano-ZnO.

Product name	Molecular formula	*m*/*z* values
Acetaldehyde	CH_3CHO	44, 43, 31, 29, 26, 15
Carbon dioxide	CO_2	44, 28, 22, 16
2-Chloro ethanol	$ClCH_2CH_2OH$	81, 83, 43, 36, 31, 27, 15
Acetic acid	CH_3COOH	60, 59, 43, 15
2-Chloro ethyl vinyl sulfide	C_4H_7SCl	122, 94, 73, 65, 45, 27
1,3-Dithiane	$C_4H_8S_2$	120, 105, 87, 74, 45
1,4-Dithiane	$C_4H_8S_2$	120, 105, 92, 73, 61, 46
1,4-Oxathiane	C_4H_8OS	104, 74, 61, 46, 34
1-Methyl-2,5-oxathiane	C_4H_8OS	104, 89, 60, 45, 35, 27, 15
Thiirane	C_2H_4S	60, 45, 34
Oxirane	C_2H_4O	44, 31, 29, 26, 15
Thietane	C_3H_6S	74, 46, 39
2,3-Dihydrothiophene	C_4H_6S	85, 71, 58, 45
1,3-Dithiolane 1 oxide	$C_3H_6OS_2$	122, 110, 106, 98, 73, 66, 46
Ethane thiol	C_2H_6S	64, 58, 47, 37, 29, 26, 15
1,3-Oxathiolane	C_3H_6OS	106, 78, 73, 64, 53, 45, 27
1,4,7-Oxa dithionane	$C_6H_{12}OS_2$	105, 90, 78, 61, 45, 164, 121
2,2-Dichloro diethyl sulphone	$C_4H_8O_2SCl_2$	127, 92, 63, 27
Bis(2-chloroethyl) disulphide	$C_4H_8S_2Cl_2$	190, 155, 128, 92, 79, 63
Hemisulfur mustard	C_4H_9OSCl	140, 141, 111, 109, 104, 73, 63, 45, 27, 29
Thiodiglycol	$C_4H_{10}O_2S$	122, 104, 91, 61, 43
2-Hydroxy ethyl vinyl sulfide	C_4H_8OS	104, 91, 61, 43
2,2-Dichloro diethyl sulphoxide	$C_4H_8OSCl_2$	174, 158, 127, 104, 63, 27
Bis(2-chloroethyl thio) methane	$C_5H_{10}S_2Cl_2$	204, 158, 127, 92, 63, 27

decontaminated in 24 h, and this observation was found to be slightly better than that observed in dark conditions (In dark, only 83% HD was decontaminated) and inferior to that observed in the case of Sun light. GC–MS data depicted the formation of hemisulfur mustard, thiodiglycol, 2-chloro ethyl vinyl sulfide, hydroxy ethyl vinyl sulfide, and minute amounts of 2,2-dichloro diethyl sulphoxide, 2,2-dichloro diethyl sulfone, etc. demonstrating the decontamination of HD through hydrolysis, elimination and photocatalytic oxidation reactions on the surface of nano ZnO particles.

Visible light activity of ZnO nanoparticles towards HD can be attributed to the presence of inherent defect sites, residual impurities, oxygen vacancies, and other irregularities within the above. They were found to be formed during the nucleation, growth, precipitation, and calcination of ZnO nanoparticles while doing synthesis.

Excited electrons move to the defect sites from conduction band through nonradiative transitions upon illumination of ZnO nanoparticles with visible light. These electrons interact with O_2 molecules and generate $O_2^{-\bullet}$ which in turn react with moisture present on the ZnO nanoparticle and further generate $OH^\bullet$. These $OH^\bullet$ reacted with HD and decontaminated it to non-toxic products. This observation (slightly better photoreactivity of ZnO nanoparticles towards HD in the presence of visible light relative to the reactions in the absence of light), visible light activity of ZnO nanoparticles is consistent with reported results [40,41].

In a similar way, experiments were conducted by illuminating with UVA light of 0.3 mW/cm^2 intensity. Relatively, UVA light has

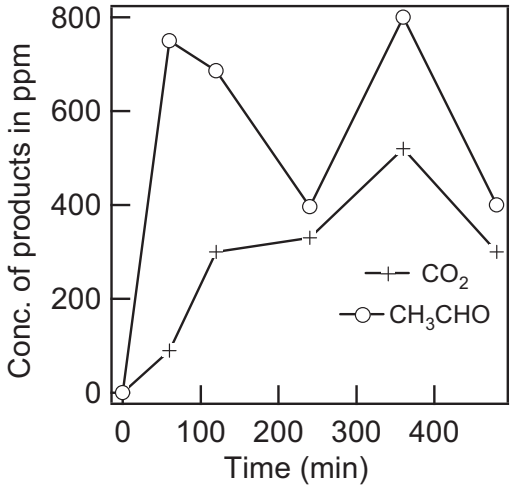

Fig. 5. Product concentration profile of HD decontaminated on nano ZnO irradiated with UVA light.

exhibited better decontamination efficiency than visible light, but interestingly it was found to be inferior to that observed in the case of Sun light. ZnO particles of average crystallite size 30 nm, have decontaminated 95% HD in 16 h (slightly lesser than Sun light, where 100% of HD was decontaminated in 12 h). Apparently, ZnO with band gap 3.2 eV is active in UVA light and hence CO_2 and acetaldehyde were formed due to degradation of HD molecules due to photocatalysis. Value of concentration of CO_2 reached 520 ppm in 6 h and it decreased to 300 ppm in 8 h (Fig. 5).

Concentration of CH_3CHO was found to be 800 ppm in 6 h, it decreased to 400 ppm in 8 h. Synergistic UVA light and nano ZnO assisted decontamination of HD also produced similar kind of products which were observed in Sun light assisted decontamination.

Based on the above observations, it was understood that $OH^\bullet$ have played predominant role in decontamination of HD in to non-toxic products in the presence of Sun light or UVA light or visible light.

Formation of hydroxyl radicals on the surface of ZnO nanoparticles in the presence of Sun light or UVA light or visible light was probed by the reactions with DMSO. ZnO nanoparticles were mixed with DMSO (1:1%, W/W) and exposed to above said radiations. After exposure, products were extracted with ethanol, concentrated and subjected to GC–MS analysis. GC–MS data indicated the formation of methane sulfonic acid ethyl ester and methane sulfonic acid as depicted by *m*/*z* values at 124, 109, 97, 79, 65, 45 and 96, 79, 65, 48, 31. Hydroxyl radical was found to react with DMSO and converted it to methane sulfonic acid, etc. This observation confirmed the formation of hydroxyl radicals and is consistent with reported method [42].

3.2. Mechanism of photocatalytic degradation of HD on ZnO nanoparticles

In absence of light, HD reacted with surface of nano ZnO slowly by means of hydrolysis and elimination reactions as indicated by GC–MS data. A reaction scheme reflecting the decontamination of HD on ZnO in dark conditions was proposed (Scheme 1).

According to this reaction scheme, HD molecules reacted with surface of ZnO in two ways, in one way they reacted with intercalated or physisorbed water molecules and surface hydroxyl groups that were present on surface of nano ZnO to form thiodiglycol. Initially, cyclic sulfonium ion was appeared to be formed that being in form (non-volatile) of salt could not be extracted out and detected by GC. In another way, HD molecules reacted with Lewis acid

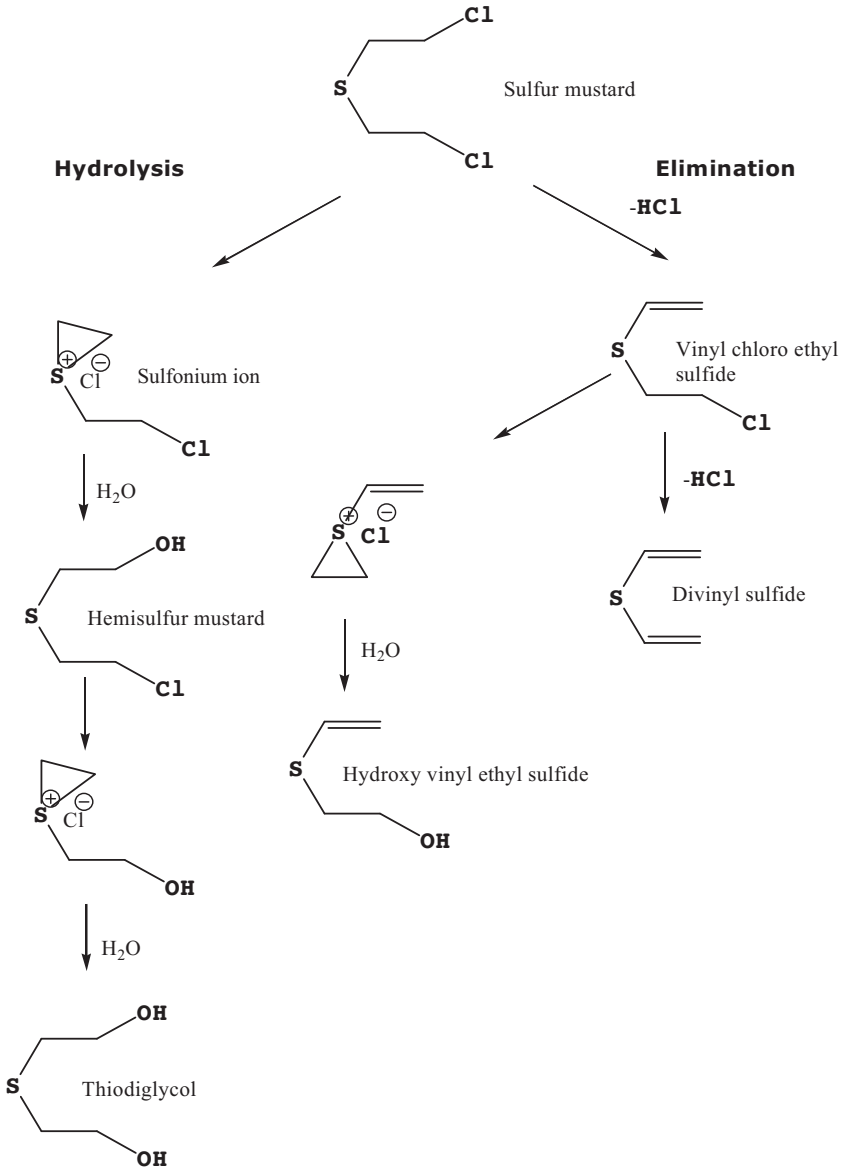

Scheme 1. Elimination and hydrolysis reactions of sulfur mustard occurring on the surface of ZnO nanoparticles.

(Zn^{2+}) sites to form surface bound alkoxy species and the same is supported by IR data. IR data indicated disappearance of band at 700 cm^{-1} (C–Cl), change of peak pattern at around 1440 and 1295 cm^{-1} (CH_2–Cl), slight change in peak intensity at ~3352 cm^{-1} (–O–H) further confirming the hydrolysis, elimination and surface complexation of HD. These reactions poison the active surface of nano ZnO and reduce the reactivity towards HD [13].

As the decontamination reactions were found to be very slow in the absence of light, photocatalysis was opted for faster decontamination removal of HD. In addition to this, it is interesting to explore how ZnO nanoparticles behave against HD when used as powder decontaminant in the natural Sun light. Apparently, data indicated faster and significant decontamination of HD due to photocatalysis in the presence of Sun light and nano ZnO, but it did not occur either in absence of ZnO or without light either Sun light or visible light or UVA light.

On the other hand, photocatalytic decontamination reaction was stimulated by light radiation. Initially, charge carriers like electrons and holes were seemed to be generated, and then migrate to the surface of photocatalyst. Holes react with moisture to form hydroxyl radicals (•OH) and protons, while electrons react with oxygen to form superoxide anion ($O_2^{-\bullet}$) radicals. These $O_2^{-\bullet}$ and •OH are extremely unstable and could have reacted with adsorbed HD molecules and decontaminated it in the presence of light.

It was revealed that, photocatalytic oxidation of HD started with sulfur radical cations, firstly the radical cation of HD reacted with superoxide anion radical or oxygen and formed HD sulfone and HD sulfoxide owing to oxidation of S atom of HD (Scheme 2). The radical cation observed to have undergone cleavage of either of C–S bonds, where, the alkyl cations reacted with water to produce alcohols and thiols as per the following reactions.

$$Cl{-}CH_2CH_2S^{+}CH_2CH_2Cl \rightarrow {}^{\bullet}SCH_2CH_2Cl + ClCH_2CH_2^{+}$$

$$^{\bullet}SCH_2CH_2Cl + H_2O \rightarrow HSCH_2CH_2Cl$$

$$ClCH_2CH_2^{+} + H_2O \rightarrow ClCH_2CH_2OH$$

This observation was also supported by GC–MS data as it had detected 2-chloro ethanol in acetonitrile extract from nano ZnO

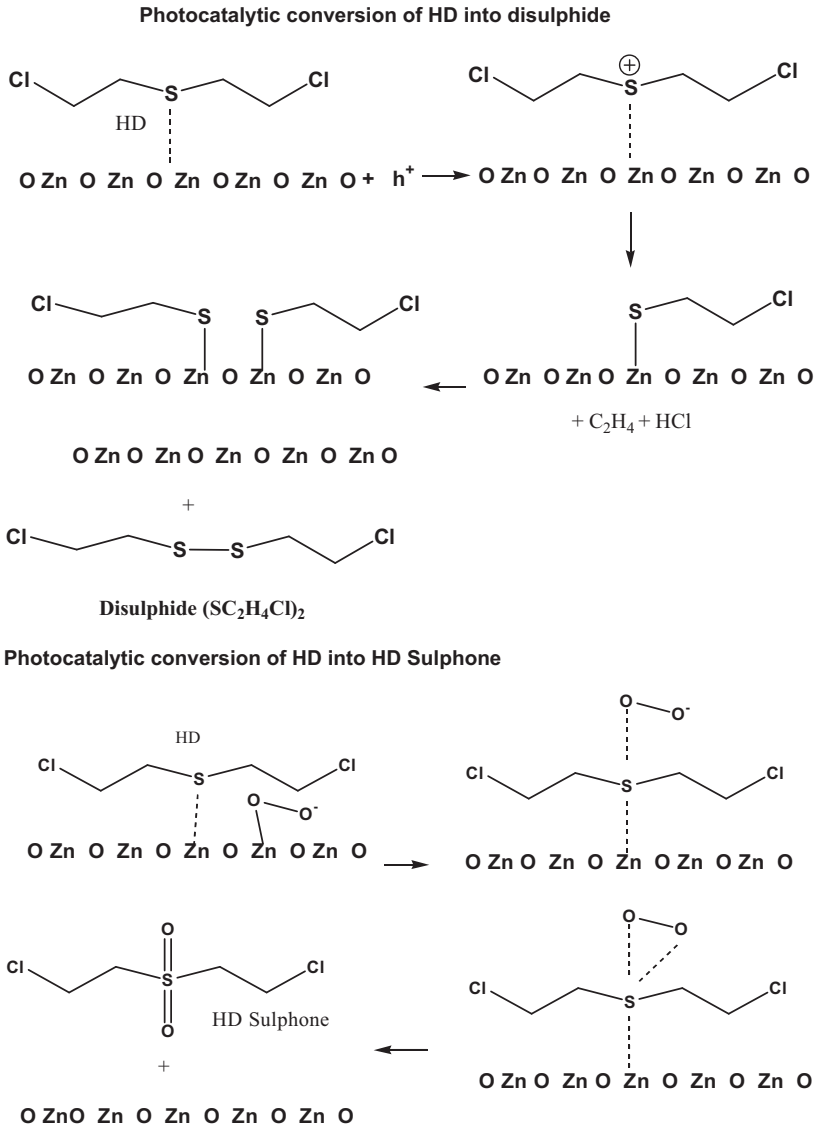

Scheme 2. Reaction mechanism indicating photocatalytic decontamination of HD on nano ZnO.

exposed to light and HD. The other route is elimination of proton from alkyl radical cation which was assisted by superoxide anion as base to form chloro ethyl vinyl sulfide, hydroxy ethyl vinyl sulfide. The thiyl radicals $ClCH_2CH_2S^{\bullet}$ formed due to photo reaction recombined giving the detected products bis(2-chloroethyl) disulfide $(-SC_2H_4Cl)_2$, bis(2-chloroethyl thio) methane $(C_5H_{10}S_2Cl_2)$. This can be ascribed to the cleavage of C–S bond.

In another way, formation of large amounts of acetaldehyde, carbon dioxide and small amounts of acetic acid, vinyl chloride, ethylene oxide, etc., can be attributed to oxidation of C atoms of HD by superoxide anion radical. The following are the proposed reactions.

$$(Cl{-}C_2H_4)_2S + O_2^{-\bullet} + H_2O \rightarrow CH_3CHO + CH_3CH_2SH$$

$$CH_3CH_2SH + O_2^{-\bullet} \rightarrow CO_2 + H_2O + H_2SO_4$$

$$CH_3CHO + O_2^{-\bullet} \rightarrow CH_3COOH$$

$$CH_3COOH + O_2^{-\bullet} \rightarrow CO_2 + H_2O$$

$$ClCH_2CH_2OH + O_2^{-\bullet} \rightarrow CO_2 + H_2O + HCl$$

$$HSCH_2CH_2OH + O_2^{-\bullet} \rightarrow CO_2 + H_2O + H_2SO_4$$

It should also be noted that, mechanism is highly complex and can also follow combinations of mechanisms such as oxidation of C atom, cleavage of C–S bond, oxidation of S atom, hydrolysis of C–Cl bond or elimination of HCl and free radical mechanisms as well. Nevertheless, based on above observations and quantities of products observed, it was understood that C–S bond cleavage had contributed to a major extent for HD photocatalytic decontamination.

3.3. Regeneration of nano ZnO

Nano ZnO was observed to be deactivated when re-used due to poisoning of catalysts i.e., formation of alkoxy species, H_2SO_4 and HCl on its surface. Initially it exhibited 95% of decontamination efficiency towards HD and it decreased to 93% when it was re used after washing with acetonitrile. Thereafter it decreased to 92% for 3rd use and then to 90% for 4th use. Whereas, ~95% of decontamination efficiency was maintained continuously for fourth time when surface of nano ZnO was treated with 30% hydrogen peroxide and UVA light followed by washing with copious amounts of water,

ethanol and dichloromethane and this observation is supported by IR data.

Formation of these species was indicated by appearance of a band at 1100 cm^{-1} (–C–O–Zn). An additional band at 1234 cm^{-1} was also observed further, indicating the formation of surface bound sulfate species. However, when treated with hydrogen peroxide and UVA light, surface was cleaned and renewed thus exhibiting better photocatalytic decontamination properties.

The IR data also showed band at 3240 cm^{-1} indicating the presence of O–H stretching vibration, a band at 1630 cm^{-1} indicating the deformation vibrations of physisorbed water. In the case of HD adsorbed on ZnO, a band at 2930 cm^{-1} indicated C–H vibration of CH_2S, bands at around 1220 cm^{-1} and 1270 cm^{-1} correspond to CH_2 vibration of CH_2–S group which are characteristics of adsorbed HD on nano ZnO. Band at 700 cm^{-1} changed due to hydrolysis of HD on ZnO. Whereas for irradiated sample (UVA or visible light or Sun light), the band pattern observed to be changed. Bands at 1126, 1200 illustrated the formation of sulphonate species and band at around 1410 cm^{-1} indicated the formation of –COOH group typical of acetic acid formed during photocatalysis of HD on nano ZnO. Further, ZnO absorbs over a larger fraction of solar spectrum due to which it made it clear that, in presence of Sun light, nano ZnO particles have exhibited superior decontamination properties when compared to that observed with UVA and visible light radiations.

4. Conclusion

Sun light assisted decontamination of HD was studied in the presence of nano ZnO particles and the data was compared with that observed in the case of UVA and visible light irradiation experiments. With the decrease of crystallite size, decontamination efficiency towards HD was found to increase. In the absence of light, hydrolysis, elimination and surface complexation reactions were found to contribute to decontamination of HD. However, in the presence of light decontamination of HD can be attributed to oxidation, cleavage of C–S bond, elimination of HCl facilitated by superoxide anion and hydroxyl radicals along with holes and electrons which were formed on the surface of nano ZnO particles due to photocatalysis in addition to the hydrolysis, elimination reactions.

Acknowledgements

Authors thank Prof. M.P. Kaushik for constant encouragement. They are also thankful to Prof. Ramesh Chandra for TEM analysis.

References

[1] L. Szinicz, Toxicology 214 (2005) 167–181.
[2] G.W. Wagner, L.R. Procell, R.J. O'Connor, M. Shekar, C.L. Carnes, P.N. Kapoor, K.J. Klabunde, J. Am. Chem. Soc. 123 (2001) 1636–1644.
[3] H. Tang, Z. Cheng, H. Zhu, G. Zuo, M. Zhang, Appl. Catal. B: Environ. 79 (2008) 323–333.
[4] R. Richards, W. Li, S. Decker, C. Davidson, O. Koper, V. Zaikovski, A. Volodin, T. Reiker, K.J. Klabunder, J. Am. Chem. Soc. 122 (20) (2000) 4921–4925.
[5] G.W. Wagner, O. Koper, E. Lucas, S. Decker, K.J. Klabunde, J. Phys. Chem. B 104 (2000) 5118–5123.
[6] M. Winter, D. Hamal, X. Yang, H. Kwen, D. Jones, S. Rajagopalan, K.J. Klabune, Chem. Mater. 21 (2009) 2367–2374.
[7] R.M. Narske, K.J. Klabunde, S. Fultz, Langmuir 18 (2002) 4819–4825.
[8] D.B. Mawhinney, J.A. Rossin, K. Gehart, J.T. Yates, Langmuir 15 (1999) 4789–4795.
[9] V.N. Sheinker, M.B. Mitchel, Chem. Mater. 14 (3) (2002) 1257–1268.
[10] E. Lucas, S. Decker, A. Khaleel, A. Seitz, S. Fultz, A. Ponce, W. Li, C. Carnes amd, K.J. Klabunde, Chem. Eur. J. 7 (12) (2001) 2505–2510.
[11] A. Kleinhammes, G.W. Wagner, H. Kulkarni, Y. Jia, Q. Zhang, L.-C. Qin, Y. Wu, Chem. Phys. Lett. 411 (2005) 81–85.
[12] G.K. Prasad, B. Singh, K. Ganesan, A. Batra, T. Kumeria, P.K. Gutch, R. Vijayaraghavan, J. Hazard. Mater. 167 (1–3) (2009) 1192–1197.
[13] G.K. Prasad, T.H. Mahato, B. Singh, K. Ganesan, P. Pandey, K. Sekhar, J. Hazard. Mater. 149 (2) (2007) 460–464.
[14] G.K. Prasad, T.H. Mahato, P. Pandey, Beer Singh, M.V.S. Suryanarayana, Amit Saxena, K. Shekhar, AIChE J. 106 (1–3) (2007) 256–261.
[15] G.K. Prasad, T.H. Mahato, B. Singh, P. Pandey, A.N. Rao, K. Ganesan, R. Vijayraghavan, AIChE J. 53 (6) (2007) 1562–1567.
[16] T.H. Mahato, G.K. Prasad, Beer Singh, K. Batra, K. Ganesan, Micropor. Mesopor. Mater. 132 (1–2) (2010) 15–21.
[17] A. Fujishima, D.A. Tryk, T.N. Rao, J. Photochem. Photobiol. C 1 (1) (2000) 1–21.
[18] K. Hashimoto, H. Irie, A. Fujishima, Jpn. J. Appl. Phys. 44 (12) (2005) 8269–8285.
[19] A. Fujishima, K. Hashimto, T. Watanbe, TiO_2 Photocatalysis, Fundamentals and Applications, BKC Press, Tokyo, 1999.
[20] F. Denny, E. Permana, J. Scott, J. Wang, D.Y.H. Pui, R. Amal, Environ. Sci. Technol. 49 (14) (2010) 5558–5563.
[21] T.E. Doll, F.H. Frimmel, Catal. Today 101 (3–4) (2005) 195–202.
[22] E.A. Kozlova, A.V. Vorontsov, Int. J. Hydrogen Energy 35 (14) (2010) 7337–7343.
[23] A.V. Vorontsov, E.N. Savinov, C. Lion, P.G. Smirniotis, Appl. Catal. B: Environ. 44 (2003) 25–40.
[24] A.V. Vorontsov, E.N. Savinov, L. Davydov, P.G. Smirniotis, Appl. Catal. B: Environ. 32 (2001) 11–24.
[25] A.V. Vorontsov, L. Davydov, E.P. Reddy, C. Lion, E.N. Savinov, P.G. Smirniotis, New J. Chem. 26 (2002) 732–744.
[26] A.V. Vorontsov, C. Lion, E.N. Savinov, P.G. Smirniotis, J. Catal. 220 (2) (2003) 414–423.
[27] N. Daneshvar, D. Salari, A.R. Khataee, J. Photochem. Photobiol. A 162 (2004) 317.
[28] S. Abbruzzetti, M. Carcellli, P. Pelagatti, D. Rominga, C. Viappiani, Chem. Phys. Lett. 344 (2001) 387.
[29] C.C. Chen, J. Mol. Catal. A: Chem. 264 (2006) 82.
[30] V. Kandavelu, H. Kastien, K.R. Thampi, Appl. Catal. B: Environ. 48 (2004) 101.
[31] A. Akyyol, H.C. Yatmaz, M. Bayramoblu, Appl. Catal. B. Environ. 54 (2004) 19.
[32] I. Poulios, I. Tsachpinis, J. Chem. Technol. Biotechnol. 74 (1999) 349.
[33] S. Sakthivel, B. Neppolian, M. Palanichamy, B. Arabindoo, V. Murugesan, Indian J. Chem. Technol. 6 (1999) 161.
[34] A. Shafaei, M. Nikazar, M. Arami, Desalination 252 (2010) 8–16.
[35] A. Nageswara Rao, B. Sivasankar, V. Sadasivam, J. Hazard. Mater. 166 (2009) 1357–1361.
[36] H. Wang, C. Xie, W. Zhang, S. Cai, Z. Yang, Y. Gui, J. Hazard. Mater. 141 (2007) 645–652.
[37] G.K. Prasad, T.H. Mahato, Beer Singh, K. Ganesan, P. Pandey, K. Sekhar, J. Hazard. Mater. 149 (2007) 460–464.
[38] T.H. Mahato, G.K. Prasad, Beer Singh, J. Acharya, A.R. Srivastava, R. Vijayaraghavan, J. Hazard. Mater. 165 (2009) 928–932.
[39] C. Hariharan, Appl. Catal. A: Gen. 304 (2006) 55–61.
[40] S. Baruah, S.S. Sinha, B. Ghosh, S.K. Pal, A.K. Raychaudhuri, J. Dutta, J. Appl. Phys. 105 (2009) 074308-1–074308-6.
[41] A. Van Dijken, E. Meulenkamp, D. Vanmaekelbergh, A. Meizerink, J. Lumin. 87–89 (2000) 454.
[42] P.L. Popham, A. Novacky, Plant Physiol. 96 (4) (1991) 1157–1160.